A family of complex potentials with real spectrum

1999 J. Phys. A: Math. Gen. 32 3105

(http://iopscience.iop.org/0305-4470/32/17/303)

J. Phys. A: Math. Gen. **32** (1999) 3105–3116. Printed in the UK PII: S0305-4470(99)99927-4

A family of complex potentials with real spectrum

F M Fernández†, R Guardiola‡¶, J Ros§ and M Znojil‖[+]

† CEQUINOR (CONICET, UNLP), Departamento de Química, Facultad de Ciencias Exactas, Universidad Nacional de La Plata, Calle 47 entre 1 y 115, Casilla de Correo 962, 1900 La Plata, Argentina

‡ Departamento de Física Atómica y Nuclear, Universidad de Valencia, Avda Dr Moliner 50, 46100-Burjassot, Valencia, Spain

§ Departamento de Física Teórica and IFIC, Universidad de Valencia, Avda Dr Moliner 50, 46100-Burjassot, Valencia, Spain

‖ Ústav jaderné fyziky AV ČR, 250 68 Řež u Prahy, Czech Republic

Received 4 December 1998

Abstract. We consider a two-parameter non-Hermitian quantum mechanical Hamiltonian operator that is invariant under the combined effects of parity and time reversal transformations. Numerical investigation shows that for some values of the potential parameters the Hamiltonian operator supports real eigenvalues and localized eigenfunctions. In contrast with other parity times time reversal symmetric models which require special integration paths in the complex plane, our model is integrable along a line parallel to the real axis.

1. Introduction

Recent analysis of the spectra of the family of Schrödinger operators with a complex parity times time reversal (PT) invariant potential [1]

$$H = -\frac{\mathrm{d}^2}{\mathrm{d}x^2} - (\mathrm{i}x)^\alpha \tag{1}$$

has raised considerable interest in such a class of operators [2–6]. The motivation for the requirement of PT (actually, complex conjugation) symmetry comes from a conjecture of D Bessis relating it to the existence of real-energy bound states (in other words, non-decaying resonances). From a practical point of view, PT symmetry is a way of selecting a specific Riemann sheet in the $(-\infty, 0)$ cut complex coordinate plane, the cut being necessary to cope with the $x = 0$ branch point of the potential.

The loss of hermiticity of H seems to imply complex energies for localized eigenstates, with $\mathrm{Im}\, E_n \neq 0$ (i.e. levels with nonzero widths), and consequently a certain rate of decay of any initially localized state. The loss of hermiticity may be mediated, e.g., by a spatial asymmetry of the potential. For example, it seems obvious that the cubic anharmonic Hamiltonian

$$H = -\frac{\mathrm{d}^2}{\mathrm{d}x^2} + x^2 + gx^3 \tag{2}$$

allows particles to escape to infinity for any real coupling $g \neq 0$.

¶ E-mail address: Rafael.Guardiola@uv.es
[+] E-mail address: znojil@ujf.cas.cz

0305-4470/99/173105+12$19.50

A deeper perturbative and Borel-summation analysis of this problem proved such an oversimplified thumb rule wrong many years ago. Calicetti *et al* [7] have shown that the spectrum of the cubic anharmonic oscillator (2) becomes *purely real* and positive at any purely imaginary coupling $g = \mathrm{i}g_I$ with $g_I > 0$. Moreover, the interpretation of the set of resonances of the Hamiltonian (2) as analogous to a set of bound states requires a suitable analytic continuation in g and/or a careful deformation of the integration path [8].

The Schrödinger equation for the Hamiltonian operator equation (1) cannot be integrated algebraically, and one has to resort to numerical methods for its analysis. Cannata *et al* [3] have found a way of generating complex Hamiltonians related to real Hamiltonians, by applying a method invented by Darboux more than 100 years ago. Unfortunately, the resulting models have a very complicated structure.

In this paper we propose a family of problems characterized by two parameters, see equation (3) below, one of them (α) playing a role analogous to the parameter α of equation (1) and the other (β) serving to *tune* the interaction thus widening the richness of the spectrum. Our study of this family will be numerical or, in other words, phenomenological, hoping that it will help a further mathematical analysis. One of the main simplifications of our model is that the required complex integration paths are lines parallel to the real axis, easy to implement and to interpret.

2. The model

We consider the two-parameter family of one-dimensional potentials

$$V_{\alpha\beta} = -(\mathrm{i}\sinh x)^\alpha \cosh^\beta x \tag{3}$$

for arbitrary real values of α and β. These functions have, in general, a branch point at $x = 0$ and we select such a branch that the real part of the potential is *symmetric* and the imaginary part *antisymmetric* with respect to the origin. Specifically, the potential will be defined by the two equations

$$x > 0 V(x) = \mathrm{e}^{\mathrm{i}\pi(2+\alpha)/2} \sinh^\alpha x \cosh^\beta x$$
$$x < 0 V(x) = \mathrm{e}^{-\mathrm{i}\pi(2+\alpha)/2} \sinh^\alpha |x| \cosh^\beta x$$

thus having an invariant Hamiltonian under the PT transformation, i.e., parity transformation and complex conjugation. This requires us to cut the complex x-plane from $x = 0$ up to $x = -\infty$, and to consider the relevant negative x values below the cut, i.e. with a small negative imaginary part or a phase $-\pi$.

The characteristic values of the potential for different values of the parameter α are shown in table 1, where we only see the region $\alpha \in [0, 4]$, because the same structure is repeated

Table 1. Variability of our PT symmetric potential with parameter α, for $x > 0$ and any real β.

α	Real part	Imaginary part
0	$V_R < 0$	$V_I = 0$
$0 < \alpha < 1$	$V_R < 0$	$V_I < 0$
$\alpha = 1$	$V_R = 0$	$V_I < 0$
$1 < \alpha < 2$	$V_R > 0$	$V_I < 0$
$\alpha = 2$	$V_R > 0$	$V_I = 0$
$2 < \alpha < 3$	$V_R > 0$	$V_I > 0$
$\alpha = 3$	$V_R = 0$	$V_I > 0$
$3 < \alpha < 4$	$V_R < 0$	$V_I > 0$
$\alpha = 4$	$V_R < 0$	$V_I = 0$

for larger values of α with period four. In all cases, both the real and imaginary parts of the potential tend to either $+\infty$ or $-\infty$ at long distances, when $x \to \pm\infty$. The value of β does not affect the main features of the potential, except for the fact that negative values of β may give rise to non-confining potentials. We exclude such cases from this paper and always consider $\alpha + \beta > 0$.

The interesting point about PT symmetric Hamiltonians

$$H = -\frac{\mathrm{d}^2}{\mathrm{d}x^2} + V_{\alpha\beta}(x) \tag{4}$$

is that they may have *localized* solutions, corresponding to real eigenvalues, which may be interpreted either as bound states or as zero width resonances.

The special case $\alpha = 2$ corresponds to a positive and confining potential, with an infinite number of bound states. It will be a suitable reference point for calculations corresponding to other values of α. We will move towards $\alpha > 2$ and $\alpha < 2$ starting from a given eigenvalue of the case $\alpha = 2$ to show the evolution of the real-energy eigenstates.

Analogously, one may take any other reference value of $\alpha = \alpha_R$ which produces a real and positive confining potential, like $\alpha_R = 6$, $\alpha_R = 10$, and so on. Selecting a different value of α_R means to consider a different eigenvalue problem, which will be labelled by that particular reference value α_R. Here we will concentrate on the case $\alpha_R = 2$ mentioned above, and also raise considerations for other values of α_R.

This family of potentials is similar to the one-parameter family $V(x) = -(\mathrm{i}x)^\alpha$ recently considered by Bender and Boettcher [1], but the exponential growth of our potentials at long distances simplifies the analysis of their properties.

3. Paths in the complex plane

By carrying out the integration of the Schrödinger equation

$$-\frac{\mathrm{d}^2\Psi(x)}{\mathrm{d}x^2} + V_{\alpha\beta}\Psi(x) = E\Psi(x) \tag{5}$$

along the real axis (see below for more details), for values of $\alpha \in [0, 4[$, one observes that there are solutions for real values of the energy E, smoothly connected with the solutions of the real potential with $\alpha = 2$. The wavefunctions are complex, and may be chosen to have a symmetric real part and an antisymmetric imaginary part. The last statement is a consequence of the PT invariance, which requires that $\Psi^*(-x)$ is a solution of the Schrödinger equation if $\Psi(x)$ is a solution for a *real* eigenvalue E. On choosing an appropriate phase factor one may then have the mentioned symmetries for the localized wavefunctions.

As discussed above, the point $\alpha = 2$ is an exception, because the Hamiltonian is separately parity and time-reversal invariant. Therefore, one can choose the wavefunctions to be real, and either symmetric or antisymmetric with respect to $x = 0$.

At $\alpha = 4$ the potential is real and everywhere negative; consequently there are no eigenstates with real eigenvalues. Real eigenvalues appear again for $\alpha \in]4, 8[$, which are smoothly connected with the case $\alpha = 6$. The same pattern is repeated at every $\alpha = 2 + 4N$, for positive integer values of N, as we increase α.

These facts are shown in figure 1, for the case $\beta = 0$. There, we clearly see the existence of two (in general, many) different problems, one centred at $\alpha_R = 2$ and the other centred around $\alpha_R = 6$. The purpose of this section is to find a path in the complex x-plane to obtain lines like the dashed one, which represents the continuation of the eigenvalue beyond the limit $\alpha = 4$.

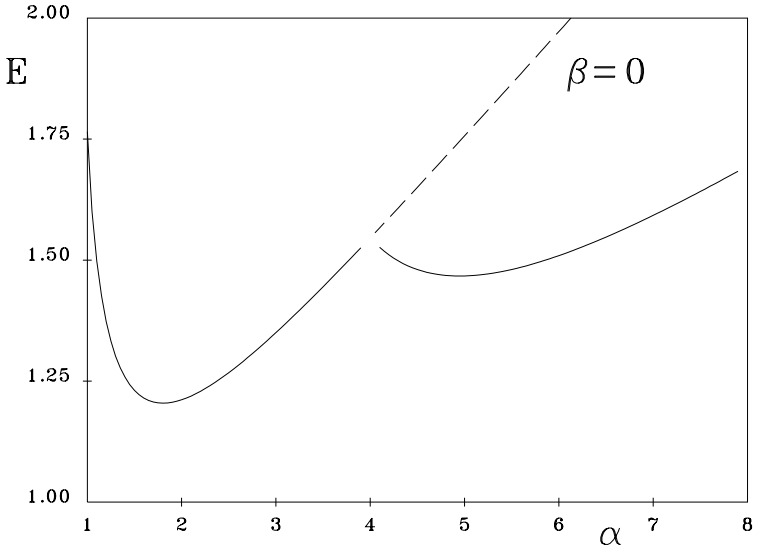

Figure 1. Integration of the Schrödinger equation along the real x-axis, for the model potential $V_{\alpha\beta}$. Only the ground-state energy is shown. The two branches correspond to solutions smoothly connected with the eigenvalues for $\alpha_R = 2$ (left curve) and $\alpha_R = 6$ (right curve). The dashed line depicts the expected eigenvalues after an appropriate analytic continuation into the complex x-plane, for the solutions smoothly connected with $\alpha_R = 2$.

The first question to consider is whether there are confined solutions. To this end we take into account the limit $x \to +\infty$ in the Schrödinger equation, where the potential is dominated by the exponential part

$$V_{\alpha\beta}(x) \to \exp[\mathrm{i}\pi(2+\alpha)/2]\exp[(\alpha+\beta)x]/2^{\alpha+\beta}.$$

One proceeds as in the WKB method assuming a general solution of the form $\Psi(x) = \exp[G(x)]$. The leading order of the asymptotic expansion for $G(x)$ is

$$G(x) \to \pm \mathrm{e}^{\mathrm{i}\pi(2+\alpha)/4}\frac{2\mathrm{e}^{(\alpha+\beta)x/2}}{2^{(\alpha+\beta)/2}(\alpha+\beta)} \tag{6}$$

where the plus and minus signs come from a square root which appears in the differential equation for $G(x)$.

Except for the particular cases $\alpha = 4N$, $N = 0, 1, \ldots$, there appears to exist a solution such that the real part of $G(x)$ is negative and its magnitude increases exponentially, suggesting a discrete set of eigenvalues with localized solutions. As mentioned above, we require $\alpha+\beta > 0$ in order to have asymptotically vanishing solutions at long distances.

The only general statement to be drawn from the above asymptotic limit is that, as far as the phase $\pi(2+\alpha)/4$ is different from a half-integer multiple of π, there are two possible asymptotic solutions, one growing and the other one decreasing at long distances; therefore, one one may expect to find one or more values of E that select the asymptotically vanishing solutions corresponding to localized states.

3.1. The $\alpha_R = 2$ family

When $\alpha = 2$ the phase factor in equation (6) is $\exp(\mathrm{i}\pi)$, and the required solution is the one with the plus sign in front of it (remember that $\Psi = \exp[G(x)]$). For $\alpha = 2 + \delta$ the phase

factor changes to $\pi + \delta\pi/4$, and the solution behaves asymptotically as

$$\Psi(x) \to \exp[[-\cos(\delta\pi/4) - \mathrm{i}\sin(\delta\pi/4)]\mathrm{e}^{(\alpha+\beta)x/2}]$$

when $x \to \infty$; i.e., the exponentially decreasing part subsists as far as $|\delta| < 2$. The farther we move from $\alpha = 2$ the slower the exponentially decreasing part approaches zero, indicating that the asymptotic regime will be reached at much larger distances.

There is a way of both moving *Asymptotia* closer and extending the integration beyond $\alpha = 4$, which consists in adding to the integration variable an imaginary component $\mathrm{i}y$ which should be negative to be consistent with the potential branch required by the PT symmetry. After the replacement $x \leftarrow x + \mathrm{i}y$ in equation (6) the phase angle of the auxiliary function G is changed to

$$\theta = \frac{\pi(\alpha+2)}{4} + \frac{y(\alpha+\beta)}{2}. \tag{7}$$

The line corresponding to $\theta = \pi$ labels the path of fastest decrease of the exponential (the *anti-Stokes* lines of [1]), and the boundaries of the region of convergence result from the solutions of $\theta = \pi \pm \pi/2$.

The optimal path corresponds to a value of y given by

$$y = \frac{(2-\alpha)\pi}{2(\alpha+\beta)} \tag{8}$$

and remains negative for any value of $\alpha > 2$, fulfilling the requirement for PT symmetry. The integration, however, may be performed for any value of y in the range

$$y_+ = \frac{(4-\alpha)\pi}{2(\alpha+\beta)}$$
$$y_- = -\frac{\alpha\pi}{2(\alpha+\beta)}$$

so that, for $\alpha < 2$ the integration should be carried out along the real x-axis to satisfy PT symmetry. The optimal and boundary values of y are plotted in figure 2. We see that without violating PT symmetry, the integration may be carried out along the real axis up to $\alpha = 4$.

Here our model differs significantly from that considered by Bender and Boettcher [1]. In their model, equation (1), the integration must be carried out along two symmetric sectors, one in the lower-right complex x-plane, and the other symmetric with respect to the imaginary axis. The optimal line is given by $x\exp(\mathrm{i}\theta)$, where $\theta = -(\alpha-2)/(\alpha+2)(\pi/2)$, in such a way that it tends to coincide with the negative imaginary axis for large values of α. In our case the displacement y remains bounded in the large-α limit, having the value $-\pi/2$.

3.2. The families for $\alpha_R = 6$ and beyond

We can carry out an analogous study for the family of potentials connected to $\alpha = 6, 10, \ldots$. For the case $\alpha = 6$ one obtains the optimal displacement

$$y = \frac{(6-\alpha)\pi}{2(\alpha+\beta)}$$

and the lower limit

$$y_- = \frac{(4-\alpha)\pi}{2(\alpha+\beta)}$$

which is suitable for the integration when $\alpha > 4$.

To extend the integration to $\alpha < 4$ we choose an alternative path given by the solution with minus sign in equation (6), leading to an optimal displacement $y = -\pi(\alpha+6)/2(\alpha+\beta)$.

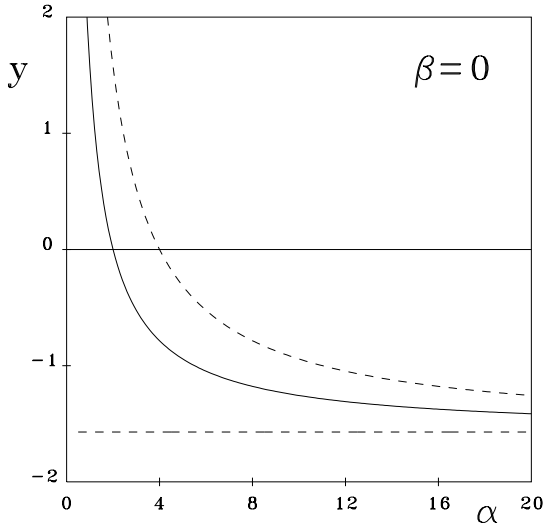

Figure 2. The continuous line represents the preferred value of the imaginary part y added to the coordinate x, for each value of α and for the family of eigenstates smoothly connected with $\alpha_R = 2$. The two dashed curves are the boundaries of the acceptable values of y.

After this discussion we clearly understand the peculiar behaviour of the lowest real eigenvalue shown in figure 1. The integration having been carried out along the real axis, the lowest eigenvalues jump from family to family when crossing the points where the potential is purely imaginary. Actually, the way of obtaining the eigenvalue by requiring that only the normalizable component survives selects the plus or minus sign in equation (6). In this way, in addition to the lack of continuity in the eigenvalues, one may also observe a sudden jump in the phase of the wavefunction (i.e. the sign of the imaginary part near 0^+) when crossing each special case mentioned above.

3.3. The role of the shift y

It is not difficult to understand the role of the change of variable $x \to x + \mathrm{i}y$ if we just carry it out explicitly in equation (5). The potential-energy function in the resulting Schrödinger equation reads

$$V_{\mathrm{eff}}(x) = V(x + \mathrm{i}y)$$

so that the new potential with the above-mentioned values of y has a dominant confining real part and a much smaller imaginary part.

The actual effect of the transformation is shown in figure 3 for three values of α. Particularly impressive is the case $\alpha = 4$ which originally was a real and negative potential, and after the transformation exhibits a dominant real confining component. The transformation of the potential guarantees the connection through the special points $\alpha = 4N$.

4. Numerical integration

The numerical calculation of the eigenvalues of the Schrödinger equation (5) with a complex potential and along a complex path, is as simple as in the case of real potentials along a real path.

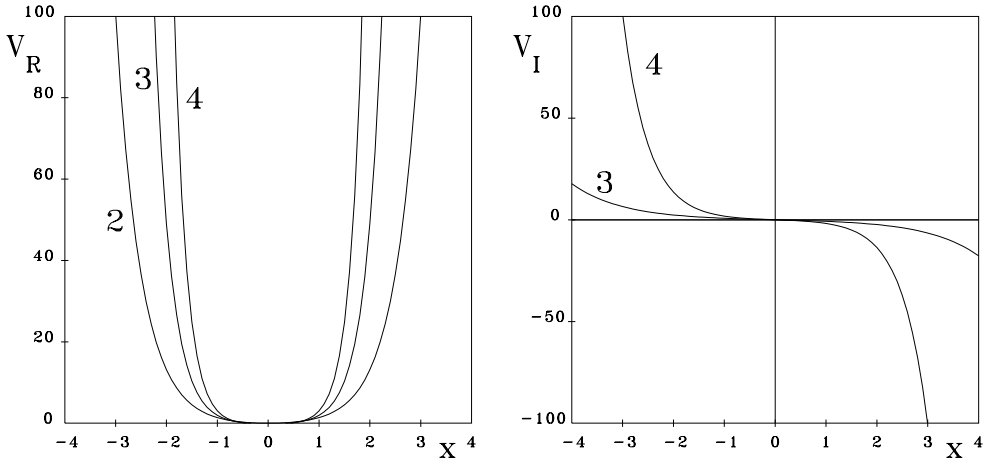

Figure 3. Real (left) and imaginary (right) parts of the effective potential obtained by shifting the real variable x to the lower part of the complex plane with the optimal y value. The potentials correspond to the phase selection appropriate for the family smoothly connected with $\alpha = 2$. The calculations were performed with $\beta = 0$ for three values of $\alpha = 2, 3$ and 4, which label the corresponding curve.

We have chosen the simplest algorithm which starts by selecting two extreme points, $X_{\min}$ and $X_{\max}$, at which the wavefunction is assumed to vanish, and discretizing this interval with a uniform integration step h, defined in terms of the number of points N as

$$h = \frac{X_{\max} - X_{\min}}{N+1}.$$

In order to preserve the PT invariance in the discretization, it is necessary to take $X_{\min} = -X_{\max}$. An integer counter k labels the mesh points as $x_k = X_{\min} + kh$. Approximating the second derivative by the second differences operator,

$$\frac{\mathrm{d}^2\Psi_k}{\mathrm{d}x^2} \simeq \frac{\Psi_{k+1} - 2\Psi_k + \Psi_{k-1}}{h^2}$$

the continuous eigenvalue problem becomes a discrete one given by a *symmetric* and *tridiagonal* matrix of dimension N and matrix elements

$$\begin{aligned} H_{ii} &= \frac{2}{h^2} + V_k \\ H_{i,i+1} &= -\frac{1}{h^2}. \end{aligned} \tag{9}$$

It is understood that $V_k = V(X_{\min} + kh + \mathrm{i}y)$ in the equation above, where y is the appropriate imaginary shift already described earlier.

The tridiagonal matrix is symmetric, but, contrary to the case of a real potential, it is not Hermitian. The roots of the determinant

$$D_N(E) = \det[H - IE] = 0$$

give the eigenvalues approximately. The calculation is greatly facilitated by the three-point recurrence relation

$$D_n(E) = D_{n-1}(E)(H_{nn} - E) - H_{n,n-1}^2 D_{n-2} \qquad n = 2, 3, \ldots, N \tag{10}$$

with the starting conditions $D_0 = 1$ and $D_1 = H_{11} - E$. This recurrence relation exhibits the same structure as in the case of a real potential, but not the same properties. In the case of a real

potential every term of the sequence is real, and the set constitutes a *Sturm sequence* [9, 10]. This property allows one to devise a simple search algorithm, combining the counting of sign changes of the sequence with the bisection method to determine efficiently the eigenvalues.

This scheme is not appropriate for our case because the potential is complex. However, an important feature of our approach is that PT symmetric potentials give rise to determinants which are polynomial functions E with real coefficients. The proof is quite simple. First one notices that the diagonal matrix elements satisfy the rule

$$H_{ii} = H^*_{N-i+1,N-i+1},$$

consequence of the PT symmetry. So, the time reversal operation T, which corresponds to changing each element of the diagonal by its complex conjugate, is equivalent to applying the parity P operation, which corresponds to changing every element of the diagonal by its symmetric with respect to the centre of the diagonal (this operation is carried out by a similarity transformation with an orthogonal matrix having all elements equal to zero with the exception of the counter-diagonal elements which are unity).

In conclusion, the determinant of $H - EI$ is real for real values of E. This is true only if $X_{\min} = -X_{\max}$, in such a way that only the determinant D_N is real, but not the terms of the sequence D_n with $n < N$. This feature allows the use of the robust bisection method to determine the eigenvalues.

In almost all cases, we have set the value of α and then determined the corresponding eigenvalue. However, in the neighbourhoods of the points where two real eigenvalues collapse into a pair of complex conjugate eigenvalues, it is more convenient to determine the value of α for a given eigenvalue. In any case, the method is simple and robust.

5. The mutual interplay of α, β and energies

Having arrived at the proper way of extending our calculations beyond the special points $\alpha = 4N$, our next step is the recomputation of figure 1 including some excited levels.

Figure 4 shows results for several levels and for the two sets smoothly connected with $\alpha = 2$ and $\alpha = 6$. The main feature of this figure is that there is a one-to-one correspondence between an eigenvalue with α close to two and an eigenvalue of the real confining potential with $\alpha = 2$. The same situation takes place at $\alpha = 6$, and it is easily proved by means of perturbation theory for α close to $2, 6, \ldots$.

Our numerical calculations suggest that there will be real eigenvalues within each family with α greater than the reference value $\alpha_R = 2$, and that for smaller values of α the real eigenvalues merge into pairs of complex conjugate values of E, until reaching the vicinity of $\alpha = 1$ where once again real eigenvalues are allowed.

Figure 5 shows in detail the special characteristics of the levels near $\alpha = 1$ for $\beta = 0$. In particular, this figure illustrates the simultaneous jump of the fourth and fifth levels into the complex plane, near $\alpha = 1.15$, and their simultaneous return to the real axis when α is slightly greater than unity. The same pattern also seems to happen for higher levels. Obviously, as far as the characteristic polynomial is real, the transition from real to complex values must be in pairs. We have not observed a similar phenomenon in the case of the set connected with $\alpha = 6$, but it may well happen for levels of energy higher than those shown in figure 4.

Up to now we have concentrated on calculations with $\beta = 0$. Figure 6 illustrates the role of the parameter β. In addition to the case $\beta = 0$, this figure also displays the lowest levels for several values of β, both positive and negative. The interesting role of β is to switch the *special* level, i.e., the level which ultimately will move around $\alpha = 1$. With its help one may choose this special level to be the first one, ($\beta = -0.25$), the third one ($\beta = 0$), the fifth one

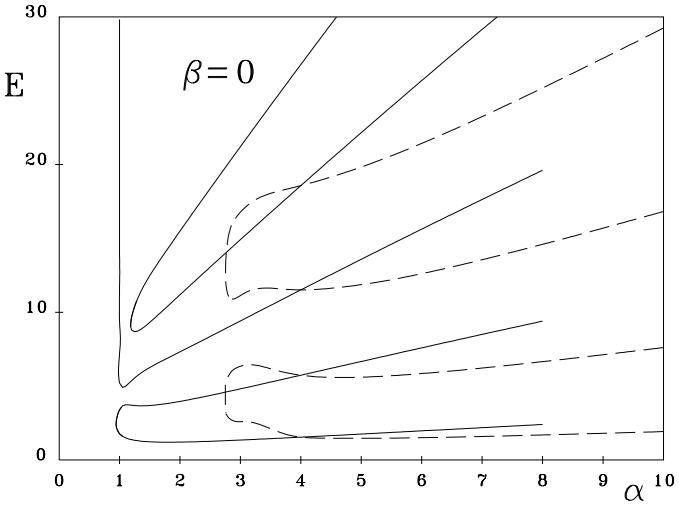

Figure 4. Spectrum of the PT invariant Hamiltonian with the potential $V_{\alpha\beta}$ and $\beta = 0$, showing several bound states corresponding to two families, one connected with $\alpha = 2$ (continuous curves) and the other connected with $\alpha = 6$ (dashed curves).

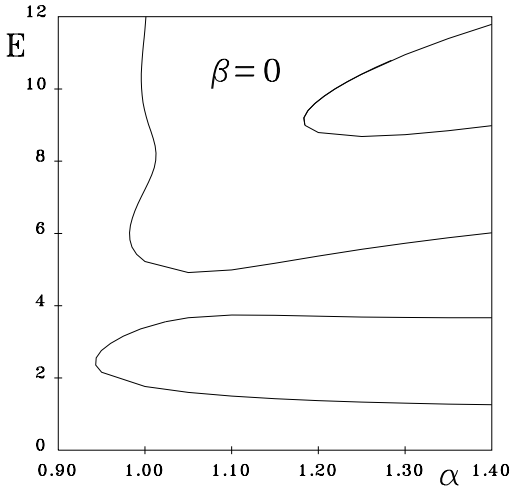

Figure 5. Enlarged view of the spectrum for $\beta = 0$ near $\alpha = 1$.

($\beta = 0.25$) and so on. Because of the special way the levels form the pairs, one should not be surprised that even levels cannot become *special* in the above-mentioned sense.

6. Quasi-algebraic study

As in our previous paper on the subject, we have also supplemented the numerical calculation with the Riccati–Padé method (RPM). When $\alpha = 2$ and $\beta = 0$ the potential-energy function is parity invariant and the RPM leads to just one Hankel determinant from which one obtains the eigenvalues [12]. The calculation is straightforward and the rate of convergence sufficiently great as shown in table 2.

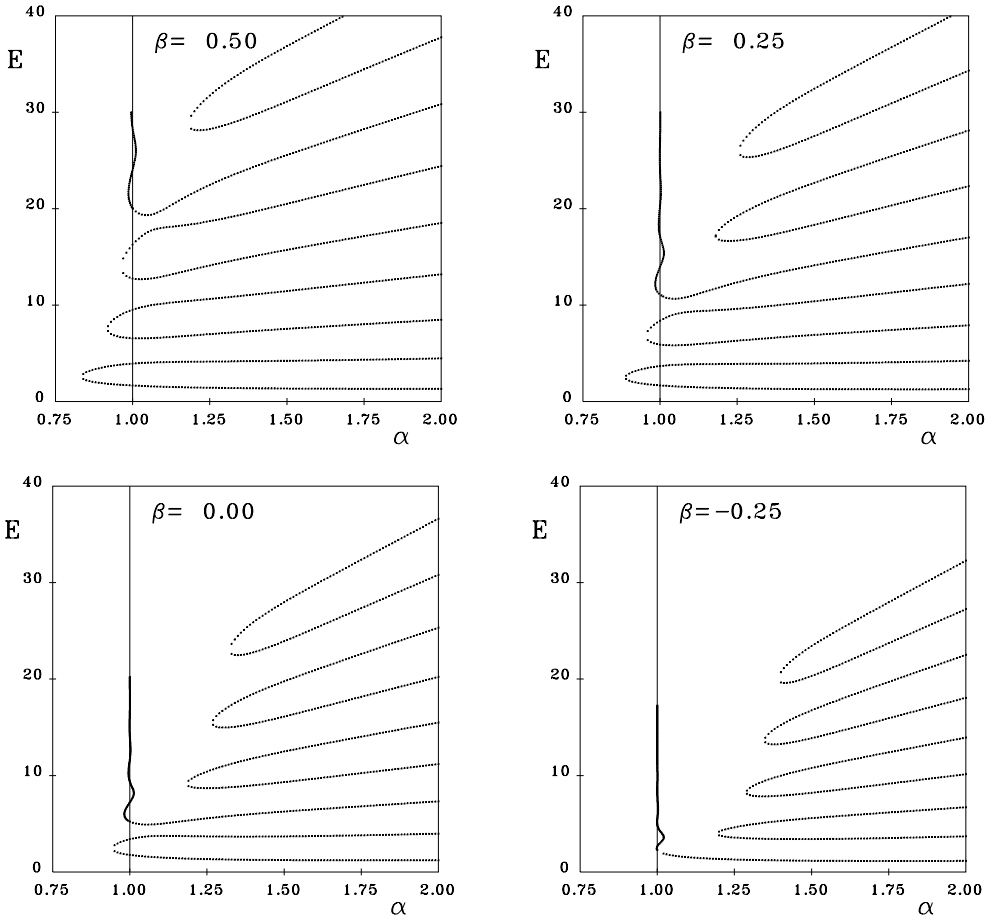

Figure 6. Several eigenvalues computed at $\beta = 0.5$, $\beta = 0.25$, $\beta = 0$ and $\beta = -0.25$.

Table 2. The RPM ground-state energy for $\beta = 0$ and $\alpha = 2$ in terms of the dimension of the Padé determinant.

D	RPM root
2	1.213 616 523
3	1.211 409 311
4	1.211 411 109
5	1.211 410 983 0
6	1.211 410 984 169
7	1.211 410 984 175 5
8	1.211 410 984 175 27

For non-Hermitian cases we change the coordinate according to $x = \mathrm{i}q$ so that the Hamiltonian operator becomes

$$-H = -\frac{\mathrm{d}^2}{\mathrm{d}q^2} + [-\sin(q)]^\alpha \cos(q)^\beta$$

and we can apply the RPM as in the case of a real Schrödinger equation. If the potential energy is an even function of q we apply the method just indicated; if it is not then the RPM leads

Table 3. The RPM ground-state energies for the non-Hermitian cases $\alpha = 1$ and $\alpha = 3$. In both cases is $\beta = 0$.

	$\alpha = 1$	$\alpha = 1$	$\alpha = 3$	$\alpha = 3$
D	E	$\mathrm{i}\Psi'(0)/\Psi(0)$	E	$\mathrm{i}\Psi'(0)/\Psi(0)$
2	1.655 005 966	1.033 573 034	—	—
3	1.765 033 153	1.095 023 981	1.385 656 774	−0.504 969 7062
4	1.765 157 398	1.095 137 449	1.349 869 536	−0.476 995 2880
5	1.765 157 246	1.095 137 384	1.350 149 473	−0.477 153 6171
6	—	—	1.350 140 759	−0.477 152 0606
Numeric	1.765 157 25	1.095 137 37	1.350 140 990	−0.477 152 00

Table 4. The RPM ground-state energies for the non-Hermitian cases $\alpha = 1$ and $\alpha = 3$ with the complex rescaled Hamiltonian. In both cases is $\beta = 0$.

D	$E(\alpha = 1)$	$E(\alpha = 3)$
2	1.765 248 635	2.609 040 864 09
3	1.765 157 328	2.595 107 274 93
4	1.765 157 255	2.595 248 416 37
5	1.765 157 255 252 31	2.595 245 998 23
6	1.765 157 255 253 36	2.595 246 050 87
7	1.765 157 255 253 358 7	2.595 246 050 34
8	1.765 157 255 253 358 74	—

to two Hankel determinants [13] from which we obtain both E and $-\mathrm{i}\Psi'(0)/\Psi(0)$. Table 3 shows results for $\alpha = 1$ and $\alpha = 3$ in excellent agreement with the numerical integration discussed above.

We have carried out the RPM calculations algebraically by means of Maple, resorting to a numerical approach just at the end in order to obtain the roots of the Hankel determinants [12, 13]. For this reason the requirement of computer memory is considerable in the case of a non-symmetric potential-energy function, and we cannot handle determinants of the same dimension as in the symmetric case. For $\beta = 0$ we have tried to overcome this problem by means of the change of coordinate $x = \mathrm{i}(u + \pi/2)$ [11] and applying RPM for symmetric potential-energy functions to the resulting Hamiltonian operator

$$-H = -\frac{\mathrm{d}^2}{\mathrm{d}u^2} + [-\cos u]^\alpha.$$

Table 4 shows results for $\alpha = 1$ and $\alpha = 3$. In the former case the result is identical (though more accurate) to the one shown in table 3; however, in the latter case we do not obtain the lowest eigenvalue but the first excited one. We have not yet being able to justify this anomalous behaviour of the RPM when $\alpha = 3$.

Acknowledgments

RG and JR are supported by DGES under contract No PB97-1139. MZ acknowledges the financial support via grants A 104 8602 (GA AV ČR) and 202/96/0218 (GA ČR).

References

[1] Bender C M and Boettcher S 1998 *Phys. Rev. Lett.* **80** 5243
[2] Bender C M and Boettcher S 1998 *J. Phys. A: Math. Gen.* **31** L273

[3] Cannata F, Junker G and Trost J 1998 *Phys. Lett.* A **246** 219
[4] Andrianov A A, Cannata F, Dedonder J P and Ioffe M V 1998 *Preprint* quant-ph/9806019
[5] Bender C M and Milton K A 1999 *J. Phys. A: Math. Gen.* **32** L87
[6] Fernández F, Guardiola R, Ros J and Znojil M 1998 *J. Phys. A: Math. Gen.* **31** 10 105
[7] Calicetti E, Graffi S and Maioli M 1980 *Commun. Math. Phys.* **75** 51
[8] Alvarez G 1995 *J. Phys. A: Math. Gen.* **27** 4589
[9] Wilkinson J H 1965 *The Algebraic Eigenvalue Problem* (Oxford: Clarendon)
[10] Golub G H and van Loan C F 1993 *Matrix Computations* (London: The Johns Hopkins University Press)
[11] Moiseyev N 1998 *Phys. Rep.* **302** 211
[12] Fernández F M and Guardiola R 1993 *J. Phys. A: Math. Gen.* **26** 7169
[13] Fernández F M and Tipping R H 1996 *Can. J. Phys.* **74** 697